



New Antimicrobial Polymeric Microspheres Containing Azomethine

Eyüp Ülke¹ · Elvan Hasanoğlu Özkan² · Dilek Nartop³ · Hatice Ögütçü⁴

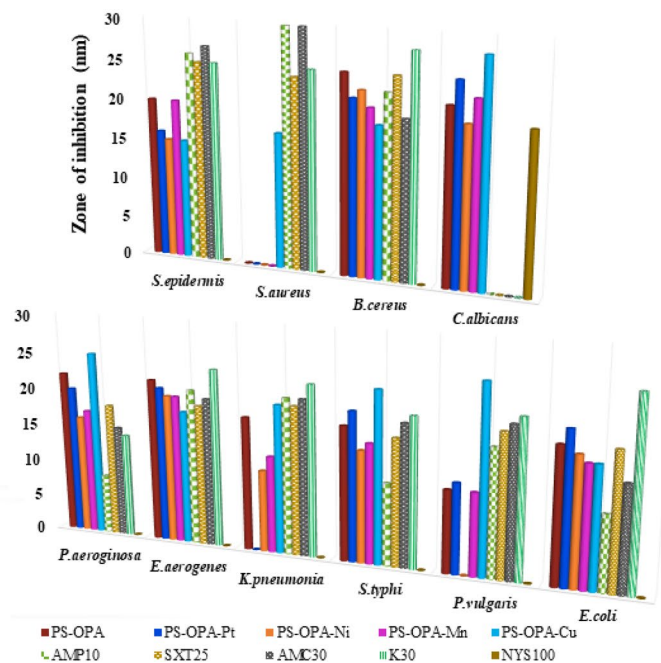
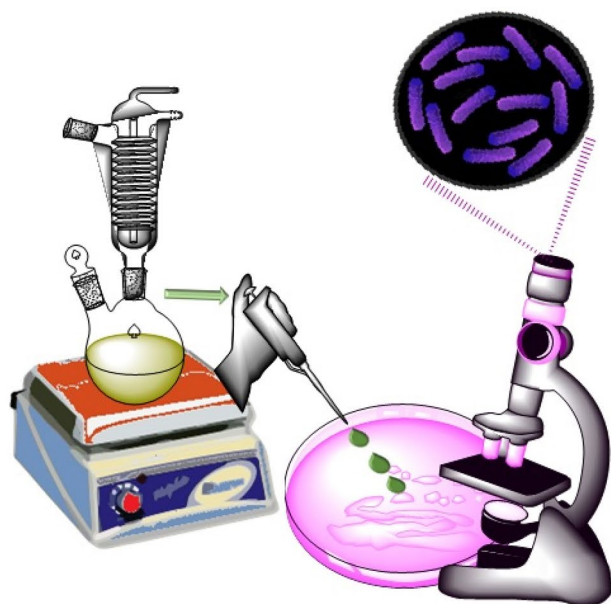
Received: 9 April 2022 / Accepted: 6 June 2022 / Published online: 24 June 2022

© The Author(s), under exclusive licence to Springer Science+Business Media, LLC, part of Springer Nature 2022

Abstract

Herein, new polymeric microspheres containing azomethine (PS–OPA, PS–OPA–Pt, PS–OPA–Ni, PS–OPA–Mn and PS–OPA–Cu) were synthesized and investigated by elemental analysis, FT-IR, SEM–EDX, TGA–DTA, UV–Vis, GPC and magnetic susceptibility. Antibacterial and antifungal activities of the synthesized polymeric microspheres were evaluated against pathogenic bacteria (*Staphylococcus epidermidis* ATCC12228, *Bacillus cereus* RSKK863, *Staphylococcus aureus* ATCC25923, *Enterobacter aerogenes*, *Pseudomonas aeruginosa* sp., *Klebsiella pneumonia* ATCC27853, *Salmonella* type H NCTC9018394, *Proteus vulgaris* RSKK96026, *Escherichia coli* ATCC1280) and yeast (*Candida albicans* Y-1200-NIH) by the well-diffusion method for potential biomedical applications. It was determined that polymeric microspheres exhibited higher inhibition effect against *B. cereus*, *E. aerogenes*, *P. aeruginosa*, *P. vulgaris* and showed higher antifungal activity than standard nystatin.

Graphical Abstract



Keywords Polymeric microspheres · Antimicrobial activity · Tris(2-aminoethyl)amine polymer-bound

✉ Elvan Hasanoğlu Özkan
ehasanoglu@gazi.edu.tr

Extended author information available on the last page of the article

1 Introduction

Schiff bases formed by the reaction between carbonyl compounds and primary amines are also known as imine ($R_1R_2C=NR_3$) or azomethine ($R_1CH=NR_2$) or compounds. Schiff bases form coordination compounds by donating electron pairs to metal ions as ligands [1]. Schiff bases and metal complexes attract attention because of some important properties such as corrosion inhibitory effects, catalytic activities, electronic properties, photoluminescence properties, detoxification activities, antimicrobial properties, herbicidal effects, thermal stability [2–8]. Schiff base complexes are also efficient photocatalytic catalysts. Sonochemical catalysis method, which is an environmentally friendly method, is the preferred method in the synthesis of various ceramic, inorganic, polymer-containing nano and micro-structured materials [9–14]. Furthermore, Schiff bases and their complexes are widely used in medicine, pharmacy, agriculture, cosmetic industry, plastics industry, dye industry, food industry [15–19].

Polymeric-Schiff bases containing an azomethine or imine group are also called polyazomethines or polyimines [20]. The usage areas of polymeric-Schiff bases and metal complexes are very common due to various properties such as electrical conductivity, optical property, antimutagenic effect, magnetic property, catalytic activity, thermal stability [21–24]. Poly-Schiff bases and their complexes are used in different industrial applications such as in wastewater treatment, gas chromatography, hydrometallurgy, solar energy systems, pesticides determination by enzyme immobilization [25–29]. Furthermore, polymeric-Schiff bases and metal complexes exhibit a broad spectrum of biological activities such as antiviral, antifungal, anti-inflammatory, antioxidant, anticancer, antimalarial, antiallergic, antipyretic, antimutagenic, antibacterial properties due to the fact that they contain azomethine bonds

[30, 31]. Therefore, the synthesis of new polymeric-Schiff bases including imine bond with biological and pharmaceutical importance is gaining importance.

In this study, new polymeric microspheres containing azomethine were synthesized by condensation reaction as novel potent antimicrobial agents. The synthesized polymeric microspheres were screened against selected pathogenic microorganisms by the well-diffusion method for investigate their antibacterial and antifungal activities.

2 Materials and Methods

2.1 Chemicals and Equipment

All chemicals were supplied from Sigma-Aldrich or Merck and were of analytical purity. Infrared spectra were measured on a Thermo Scientific Nicolet IS5 Fourier Transform Infrared Spectrophotometer (FT-IR) at $4000\text{--}400\text{ cm}^{-1}$ using ATR. Elemental analyses were performed on a Thermo Scientific Flash 2000 model CHNS-O elemental analyzer. Gel permeation chromatography (GPC) measurements were performed by a Waters 1500 Series GPC system. Scanning electron microscopy and energy dispersive X-ray (SEM-EDX) images were taken using a Quanta FEG 250 device. Thermal gravimetric analysis (TGA) was recorded by a Shimadzu DTG 60H-DSC 60 model thermal analyzer. Ultraviolet-Visible (UV-Vis) absorption spectra were obtained using a UV-1800 ENG240V, SOFT model spectrophotometer. Magnetic measurements were performed with a Sherwood Scientific MKI model Evans magnetic susceptibility device.

2.2 Synthesis of PS-OPA

The polymeric microsphere containing azomethine was prepared as shown in Fig. 1. PS-OPA polymer was synthesized by the condensation reaction of polymer bound

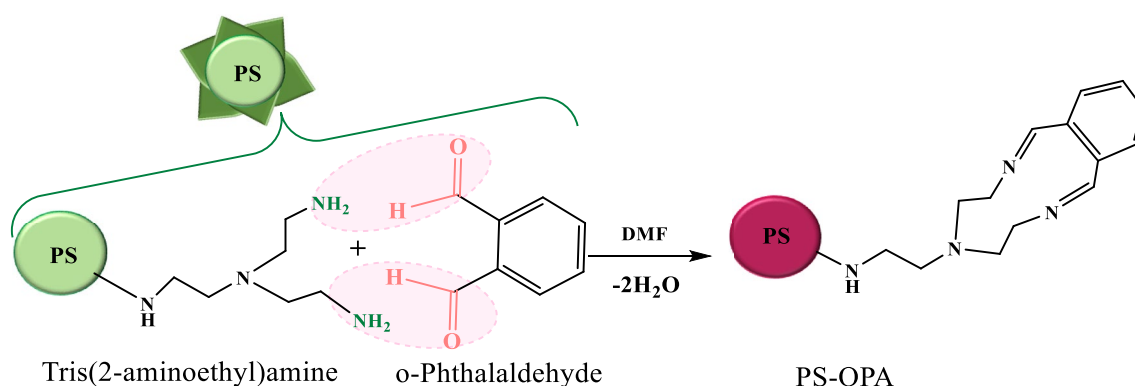


Fig. 1 Schematic representation of synthesis polymeric microsphere

tris(2-aminoethyl)amine (0.5 mmol) and *o*-phthalaldehyde (0.5 mmol). A solution of the tris(2-aminoethyl)amine polymer-bound [3.5–5 mmol/g N loaded, 200–400 mesh] in 15 mL of *N,N*-dimethylformamide (DMF) was prepared. A solution of *o*-phthalaldehyde in DMF (15 mL) was then added to polymer solution. The mixture was stirred and heated for 3 h under reflux at 70 °C. The solution was cooled to the room temperature, purified with acetone and filtered. It was then dried in an oven for 24 h.

2.3 Synthesis of Polymeric Microspheres (PS–OPA–Pt, PS–OPA–Ni, PS–OPA–Mn and PS–OPA–Cu)

All the polymeric microspheres were prepared by the same general procedure as shown in Fig. 2. PS–OPA–Pt, PS–OPA–Ni, PS–OPA–Mn and PS–OPA–Cu polymeric microspheres were synthesized by the reaction of polymer bound tris(2-aminoethyl)amine (0.5 mmol), *o*-phthalaldehyde (0.5 mmol) and metal salts (0.5 mmol) with template method. Polymeric microspheres were synthesized from polymer bound tris(2-aminoethyl)amine (0.5 mmol), *o*-phthalaldehyde (0.5 mmol) and metal salts by template method. A solution of the tris(2-aminoethyl)amine polymer-bound [3.5–5 mmol/g N loaded, 200–400 mesh] in 15 mL of *N,N*-dimethylformamide was prepared. A solution of *o*-phthalaldehyde in DMF (15 mL) was added to polymer solution. The mixture was stirred and heated for 3 h under reflux at 70 °C. A solution of the metal salt (platinum(II)chloride or nickel(II)acetate tetrahydrate or manganese(II)acetate or copper(II)acetate) in DMF (10 mL) was then added to the mixture and stirred for a further 4 h under reflux. The solution was cooled to the room temperature, purified with acetone and filtered. It was then dried in an oven for 24 h.

2.4 Antimicrobial and Antifungal Assay

To examine the antimicrobial activities of the polymeric microspheres, the well-diffusion method was used [32]. For this purpose, *Staphylococcus epidermidis* ATCC12228, *Bacillus cereus* RSKK863, *Staphylococcus aureus* ATCC25923, *Enterobacter aerogenes*, *Pseudomonas eruginosa* sp., *Klebsiella pneumonia* ATCC27853, *Salmonella type H* NCTC9018394, *Proteus vulgaris* RSKK96026, *Escherichia coli* ATCC1280 and *Candida albicans* Y-1200-NIH were selected as pathogenic bacterial cultures.

In this method, dimethylformamide was used as solvent control. It was determined that DMF had no antimicrobial activity against any of the tested organisms. All the polymeric microspheres were stored dry at room temperature and solved (3.5 µg/mL) in DMF. Pathogenic microorganisms were incubated in Nutrient Broth agar (10^6 CFU/mL) for 24 h at 37 °C. After the incubation, these cultures were homogenized by adding to Mueller-Hinton Agar (MHA) cooled to 45 °C. The agars were then poured into sterile petri dishes and were cooled. Then, holes of 6 mm diameter were pierced in these agars and the synthesized polymeric microspheres were added into these bores. The plates were then incubated in an oven at 37 °C for 24 h. After the incubation, the zone of inhibition was measured for each compound and the average of the activity values performed with two repetitions was taken.

In addition, pathogenic bacteria cultures and yeast were compared with standard antibiotics and anticandidal: ampicillin (AMP10), kanamycin (K30), sulphamethoxazole (SXT25), amoxicillin (AMC30) and nystatin (NYS100).

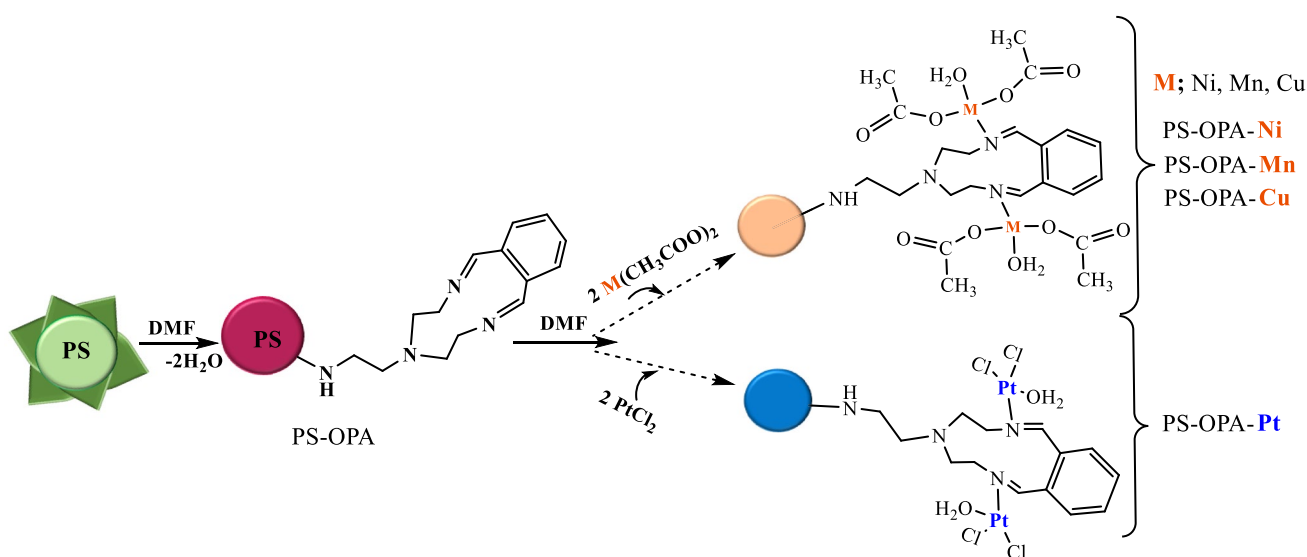


Fig. 2 Schematic representation of the synthesis of M^{2+} -attachment polymeric microspheres

3 Results and Discussion

3.1 Characterization of Polymeric Microspheres (PS-OPA, PS-OPA-Pt, PS-OPA-Ni, PS-OPA-Mn and PS-OPA-Cu)

The analytical data and some physical properties of polymeric microspheres containing azomethine are presented in Table 1.

The values of weight average molecular weight (M_w), number average molecular weight (M_n) and polydispersity index (PDI) giving the molecular weight distribution (M_w/M_n) were determined by the gel permeation chromatography [33]. The values of weight average molecular weight were also obtained by the elemental analysis.

Some characteristic infrared spectral data for polymeric microspheres containing azomethine are presented in Table 2 and are shown in Fig. 3. For all polymeric microspheres, the peaks observed in the ranges 1588–1657 cm^{-1} were predicted to be azomethine groups (CH=N) resulting from the addition of aldehydes to polymers containing amine groups. The $\nu(\text{CH})$ aromatic, $\nu(\text{CH})$ aliphatic, and $\nu(\text{C}=\text{C})$ ring absorption bands were appeared in the 3010–3192 cm^{-1} , 2880–2948 cm^{-1} and 1542–1579 cm^{-1} regions, respectively. For PS-OPA-Pt, PS-OPA-Ni,

PS-OPA-Mn and PS-OPA-Cu polymers, $\nu(\text{M}-\text{N})$ weak stretching vibrations were not determined. $\nu(\text{M}-\text{O})$ weak stretching vibrations were appeared in the range 560–582 cm^{-1} , respectively. These bands are foreseen as an indication of the coordination of the metal ion with the imine group [34–37]. Also, $\nu(\text{H}_2\text{O})$ vibrations were determined in the region 3300–3385 cm^{-1} .

The electromagnetic spectra data for polymeric microspheres containing azomethine are presented in Table 3 and are shown in Fig. 4. For all polymeric microspheres, the $n \rightarrow \pi^*$ transitions belonging to the imine group and the $\pi \rightarrow \pi^*$ transitions belonging to the aromatic ring were observed in the ranges 333–330 nm and 257–259 nm, respectively. For PS-OPA-Pt polymer, the peaks at 435 nm and 519 nm belonging to the d-d transition of the square plane Pt(II) complex were detected [34, 38]. Additionally, according to the magnetic susceptibility measurement, it was determined that PS-OPA-Pt polymer showed diamagnetic property. This result is confirmed that the polymer is in square plane geometry. For PS-OPA-Ni polymer, the absorption bands attributed to ligand-to-metal charge-transfer transition (LMCT) of the square plane Ni(II) complex were appeared in 320 and 376 nm. The band assigned to d-d transition of the square plane Ni(II) complex were also appeared in 493 nm [39]. Additionally, according to the magnetic susceptibility measurement, it was determined

Table 1 The analytical data and some physical properties of polymeric microspheres

Compound	Chemical Formula, ($*M_w$), Colour	(M_w, M_n) PDI	Elemental analysis (calc.) %				
			C	H	N	O	Metal
PS-OPA	$[(\text{C}_{10}\text{H}_{14}\text{N}_2)(\text{C}_{22}\text{H}_{26}\text{N}_4)_2]$, (854), Red brown	(896, 882) 1.02	76.60 (75.84)	7.75 (7.78)	15.65 (16.38)	–	–
PS-OPA-Pt	$[(\text{C}_{14}\text{H}_{24}\text{N}_4)(\text{C}_{22}\text{H}_{30}\text{N}_4\text{O}_2\text{Cl}_4)\text{Pt}_2]_2$, (2076), Brown	(2119, 2018) 1.05	34.02 (33.54)	4.21 (4.08)	8.14 (8.09)	3.85 (3.08)	36.53 (37.56)
PS-OPA-Ni	$[(\text{C}_{14}\text{H}_{24}\text{N}_4)(\text{C}_{30}\text{H}_{38}\text{N}_4\text{O}_{10})\text{Ni}_2]_2$, (1710), Olive-green	(1767, 1651) 1.07	50.99 (51.90)	6.03 (5.89)	10.11 (9.82)	19.00 (18.69)	13.92 (13.71)
PS-OPA-Mn	$[(\text{C}_{14}\text{H}_{24}\text{N}_4)(\text{C}_{30}\text{H}_{38}\text{N}_4\text{O}_{10})\text{Mn}_2]_2$, (1696), Mustard color	(1624, 1562) 1.04	50.96 (52.36)	6.03 (5.94)	10.07 (9.90)	18.09 (18.85)	14.86 (12.95)
PS-OPA-Cu	$[(\text{C}_{14}\text{H}_{24}\text{N}_4)(\text{C}_{30}\text{H}_{38}\text{N}_4\text{O}_{10})\text{Cu}_2]_2$, (1730), Cyan	(1711, 1614) 1.06	51.93 (51.32)	6.11 (5.82)	9.95 (9.71)	17.50 (18.48)	15.50 (14.68)

$*M_w$, weight average molecular weight (values are according to elemental analysis)

$M_w = M_n$ According to GPC

Table 2 Important IR vibration frequencies (cm^{-1}) of polymeric microspheres

Compound	$\nu(\text{H}_2\text{O})$	$\nu(\text{CH}=\text{N})$	$\nu(\text{C}=\text{C})_{\text{aro}}$	$\nu(\text{CH})_{\text{aro}}$	$\nu(\text{CH})_{\text{alp}}$	$\nu(\text{M}-\text{O}) / \nu(\text{M}-\text{N})$
PS-OPA	–	1657, 1613	1567	3010	2880	–
PS-OPA-Pt	3385	1647, 1602	1576	3192	2930	568 / n
PS-OPA-Ni	3352	1590	1547	3068	2948	575 / n
PS-OPA-Mn	3450	1651	1579	3120	2936	582 / n
PS-OPA-Cu	3440	1588	1542	3099	2900	560 / n

n not determined

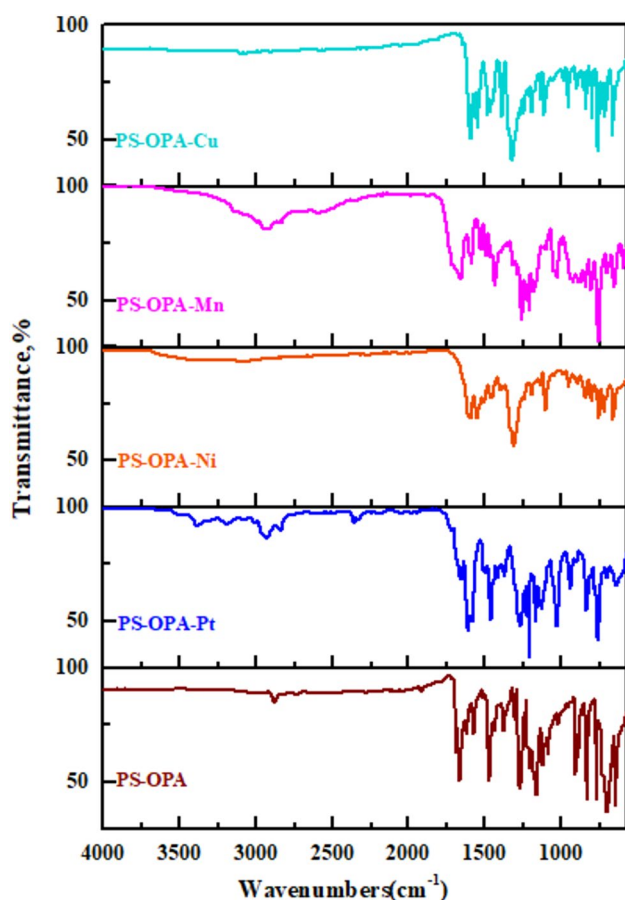


Fig. 3 FT-IR of polymeric microspheres

that PS-OPA-Ni polymer showed diamagnetic property. This result is confirmed that the the polymer is in square plane geometry [40]. For PS-OPA-Mn polymer, d-d transition was not observed in the UV-Vis spectrum. The absence of d-d transition between 600–800 nm is an indication of tetrahedral geometry [41, 42]. Additionally, the

value of magnetic susceptibility of PS-OPA-Mn polymer was found 5.89 BM. It is confirmed that the the polymer is in tetrahedral geometry with five unpaired electrons [2]. For PS-OPA-Cu polymer, the peak at 548 nm belonging to the d-d transition of the square plane Cu(II) complex were determined [37]. Additionally, the value of magnetic susceptibility of PS-OPA-Cu polymer was found 1.75 BM. It is confirmed that the polymer is in square plane geometry with one unpaired electrons [43].

SEM-EDX analysis results for polymeric microspheres containing azomethine are shown in Fig. 5. The SEM images which provide information about the morphological features, showed that the spherical structures of the polymeric microspheres are preserved after modification. Also, the EDX analysis data confirmed the basic composition of the polymers.

The thermal analysis results for polymeric microspheres containing azomethine are presented in Table 3 and are shown in Fig. 6. According to the thermal degradation curves, it was observed that PS-OPA polymeric microsphere decomposed in one-step weight. The values of initial (T_i) and finally (T_f) decomposition temperature were determined as 292 °C and 555 °C, respectively. It was observed that PS-OPA-Pt polymeric microsphere decomposed in two-step weight. In the first step, the values of T_i and T_f decomposition temperature were determined as 69 °C and 473 °C, respectively. In the second step, the values T_i and T_f were determined as 488 °C and 569 °C, respectively. It was determined that PS-OPA-Ni, PS-OPA-Mn and PS-OPA-Cu polymeric microspheres exhibited three-step weight. In the first step, the values T_i and T_f were observed in the ranges 44–108 °C and 304–389 °C, respectively. In the second step, the values T_i and T_f were observed in the ranges 339–419 °C and 419–570 °C, respectively. In the third step, the values T_i and T_f were observed in the ranges 420–671 °C and 531–763 °C, respectively. The high decomposition

Table 3 Thermal analysis data and UV-Vis spectrum values (nm, $\epsilon \times 10^4$)

Compound	Step	T_i (°C)	T_f (°C)	Residue mass at 800 °C (wt%)	Charge transfer transition / d-d transition
PS-OPA	1st	292	555	9.85	–
PS-OPA-Pt	1st	69	473	1.77	–
	2nd	488	569		435 (1328)/ 519 (1250)
PS-OPA-Ni	1st	76	346	4.52	320 (1289)/376 (984)
	2nd	385	486		493 (427)
	3rd	508	593		
PS-OPA-Mn	1st	108	304	5.25	–
	2nd	339	419		–
	3rd	420	531		
PS-OPA-Cu	1st	44	389	10.34	–
	2nd	419	570		548 (859)
	3rd	671	763		

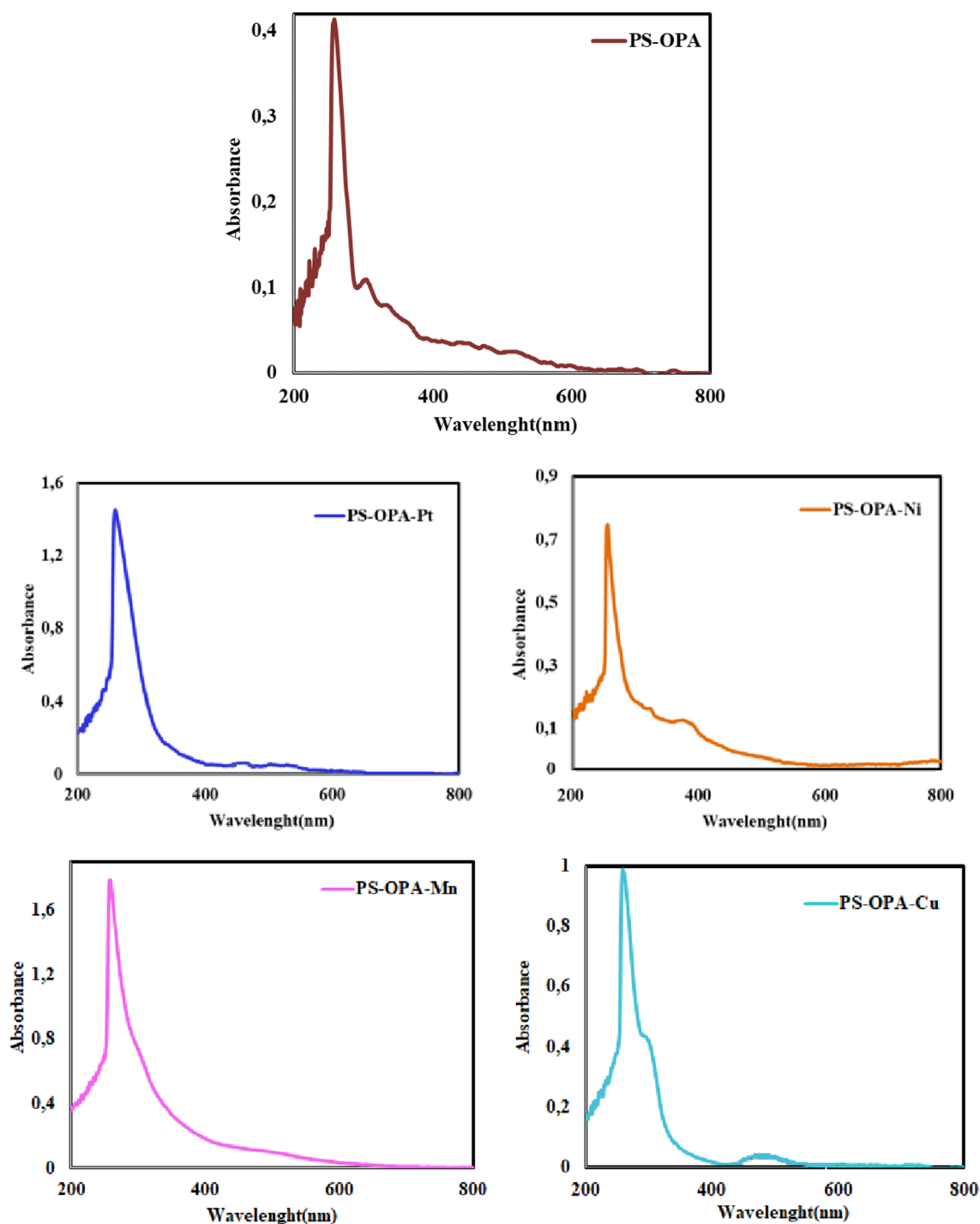


Fig. 4 UV-Vis spectra of polymeric microspheres

temperatures indicated that all polymeric microspheres have thermal stability. It was observed that newly synthesized polymeric microspheres were as stable as or more stable than the polymers obtained in our previous studies [44–46]. The percentage of residual solid in polymers

matrix at final temperature was determined to be in the ranges 1.77–10.34%.

For the antimicrobial and antifungal activity of polymeric microspheres containing azomethine, photographs of inhibition regions and graphical illustration of pathogenic bacteria

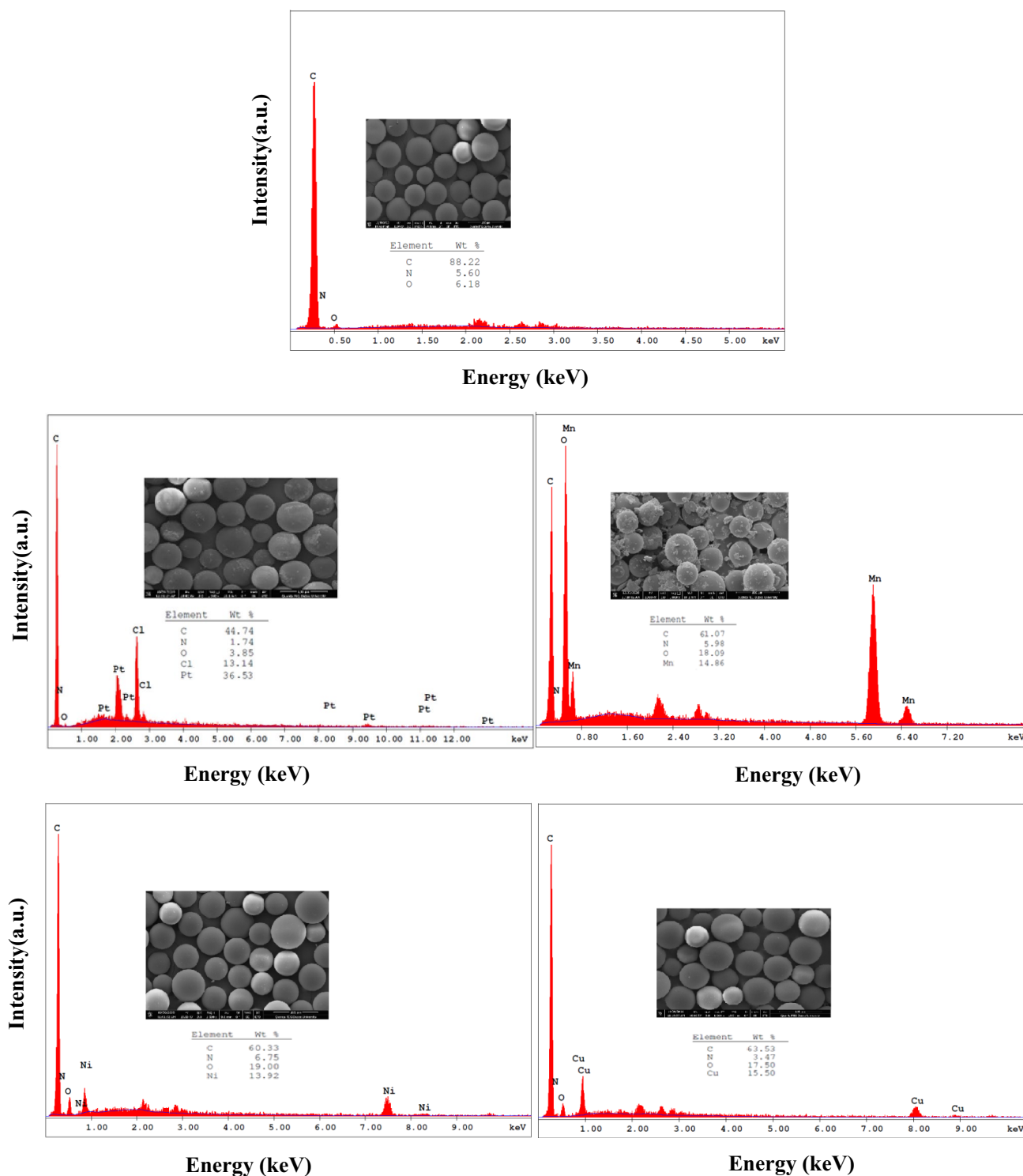


Fig. 5 SEM–EDX analysis of polymeric microspheres

are shown in Figs. 7, 8 and 9. The polymeric microspheres were screened in vitro for biological activity against some selected disease-causing pathogenic strains. Selected Gram-positive bacteria were *S. epidermidis*, *B. cereus*, *S. aureus*, Gram-negative bacteria were *E. aerogenes*, *P. eruginosa*

sp., *K. pneumonia*, *S. type H*, *P. vulgaris*, *E. coli* and yeast was *C. albicans*. It was determined that the polymers and antibiotics showed varying degrees of inhibitory activity on the growth of the tested different pathogenic strains. All polymeric microspheres exhibited the highest antibacterial

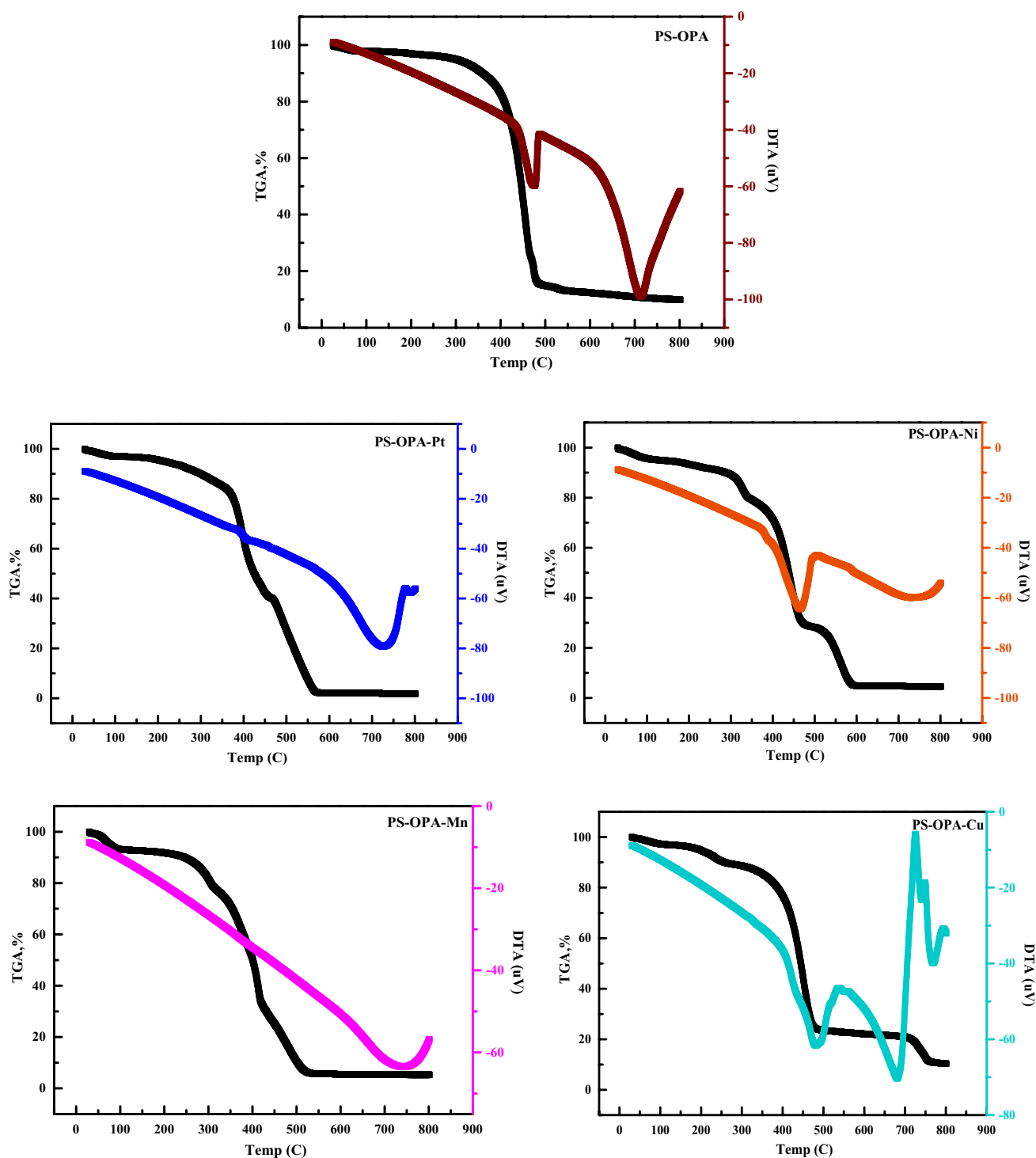
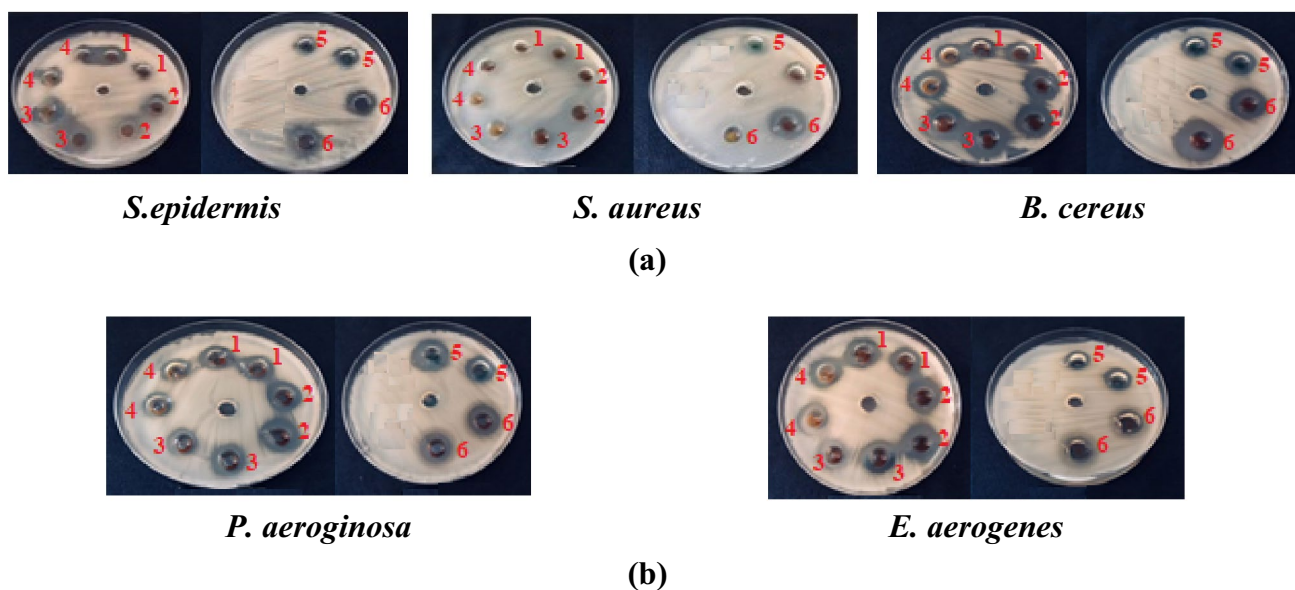


Fig. 6 TGA-DTA curves of polymeric microspheres

activity against *B. cereus* among Gram-positive bacteria. PS-OPA was the most effective among them. *B. cereus* is a Gram-positive bacterium that causes some foodborne epidemic diseases such as diarrhea, vomiting and nausea [47]. PS-OPA, PS-OPA-Pt, PS-OPA-Ni and PS-OPA-Mn

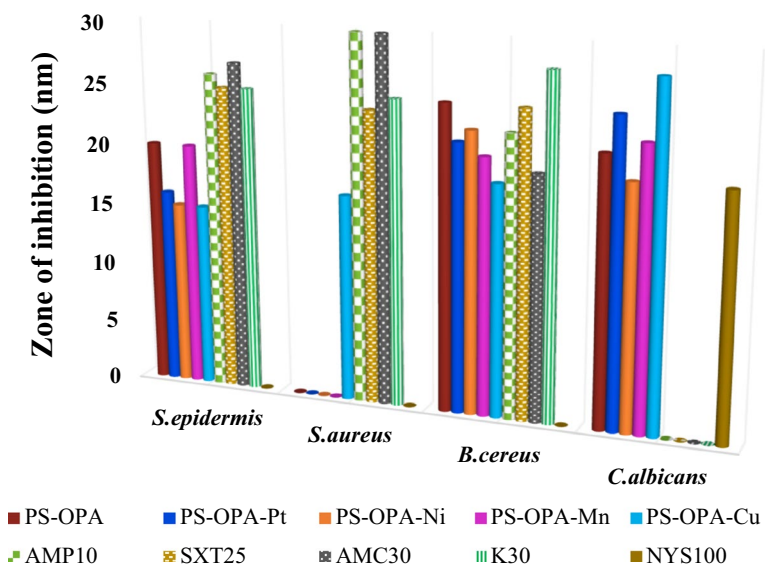
polymeric microspheres exhibited the highest antibacterial activity against *E. aerogenes* among Gram-negative bacteria. PS-OPA was the most effective among them. *E. aerogenes* is an opportunistic gram-negative bacterium that causes urinary and respiratory tract infections in immunocompromised



¹[PS-OPA], ²[PS-OPA-Pt], ³[PS-OPA-Ni], ⁴[PS-OPA-Mn], ⁵[PS-OPA-Cu]

Fig. 7 Photographs of inhibition zones (mm) of pathogenic Gram(+) (a) and Gram(–) bacteria and yeast (b)

Fig. 8 Graphical illustration of Gram(+) pathogens bacteria (*S. epidermis*, *S. aureus*, *B. cereus*), yeast (*C. albicans*) and standard reagents



individuals and patients on mechanical ventilation [48]. PS-OPA also showed high inhibitory effect against *P. aeruginosa*. In particular, it was more effective than all standard antibiotics tested against *P. aeruginosa*. This Gram-negative bacterium is an opportunistic pathogen that causes burn injuries, urinary tract infections, wounds, corneal ulcers [49]. PS-OPA-Cu exhibited the highest antibacterial activity against *P. aeruginosa* and *P. vulgaris* among Gram-negative bacteria. *P. vulgaris* is a Gram negative bacterium that causes kidney stone formation, urinary tract infections,

lung infections, anaerobic infections (tetanus) [50]. Particularly, PS-OPA-Cu was more effective than all standard antibiotics tested against *S. typhi* H. It is a Gram negative bacterium that causes enteric fever (typhoid) [51]. Additionally, PS-OPA-Pt polymer showed a higher inhibitory effect than all standard antibiotics and tested against *P. aeruginosa*. Additionally, pathogenic bacteria strains and yeast were compared with standard antibiotics and anticandidal (ampicillin, kanamycin, sulphamethoxazole, amoxicillin and nystatin). PS-OPA-Pt, PS-OPA-Mn and PS-OPA-Cu

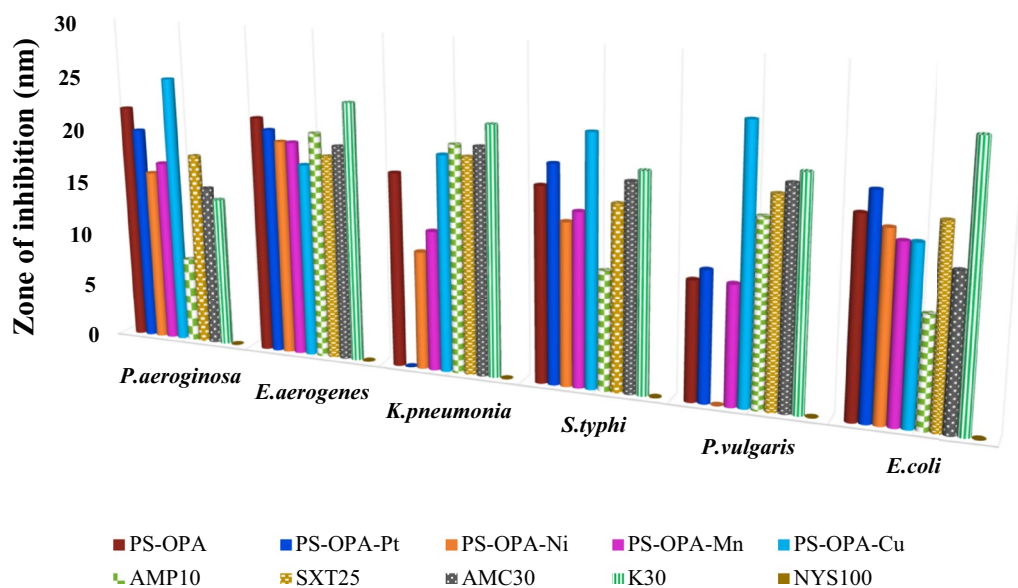


Fig. 9 Graphical illustration of Gram(−) pathogenic bacteria (*P. aeruginosa*, *E. aerogenes*, *K. pneumonia*, *S. typhi*, *P. vulgaris* and *E. coli*) and standard reagents

polymers showed higher antifungal activity against than standard nystatin anticandidal, while PS–OPA–Ni polymer similar antifungal activity to standard nystatin anticandidal. It is an antifungal drug used for the prevention of *Candida* infections [52]. *C. albicans* is an opportunistic yeast that is seen in the genitourinary and gastrointestinal systems [53].

According to the biological activity results, it was determined that polymeric microspheres inhibited the growth of test bacteria different degrees and showed good antibacterial and antifungal activity against these pathogenic microorganisms. It was observed that the polymeric microcircular had a higher inhibition effect against *B. cereus* among Gram(+) bacteria and against *E. aerogenes*, *P. aeruginosa* and *P. vulgaris* among Gram(−) bacteria. It was observed that all polymeric microspheres had a higher inhibition effect, especially against Gram(−) bacteria. According to the findings, it can be predicted that all polymeric microspheres can be recommended as biologically active compounds. The synthesized polymeric microspheres have high molecular weight and contain diimine groups that act as good chelating agents. Therefore, the synthesized polymeric microspheres have more effective antibacterial properties than the antibacterial monomer [46, 54–56].

4 Conclusions

Herein, new polymeric microspheres containing azomethine were synthesized by condensation reaction as potential antimicrobial agents and characterized by spectroscopic methods. It was determined that all polymeric microspheres were

thermally stable compounds with high decomposition temperatures. Antibacterial and anticandidal activities of polymeric microspheres were investigated *in vitro* against some pathogens causing disease. It was determined that polymeric microspheres showed a high inhibition effect against selected pathogenic strains when compared with standard antibiotics. It was determined that polymeric microspheres had a higher inhibition effect, especially against *B. cereus*, *E. aerogenes*, *P. aeruginosa* and *P. vulgaris*. As a result, it is possible to say that polymeric microspheres can be recommended as compounds with antimicrobial drug potential. In the future, studies of antimutagenic activity evaluation, enzyme immobilization, and qualitative enzymatic determination of insecticides can be carried out on the obtained polymeric microspheres. The conductivity of the polymeric microspheres can also be investigated due to containing π -linked aromatic rings.

Acknowledgements The authors thank Düzce University for equipment support.

Funding The authors have not disclosed any funding.

Declarations

Conflict of interest The authors report no declarations of interest. The authors alone are responsible for the content and writing of the paper.

References

1. M.S. More, P.G. Joshi, Y.K. Mishra, P.K. Khanna, Metal complexes driven from Schiff bases and semicarbazones for

- biomedical and allied applications: a review. *Mater. Today Chem.* **14**, 1–22 (2019)
2. S. Bal, S.S. Bal, Cobalt (II) and Manganese (II) complexes of novel schiff bases, synthesis, characterization, and thermal, antimicrobial, electronic, and catalytic features. *Adv. Chem.* **2014**, 1–12 (2014)
 3. H. Kommera, S. Gómez-ruiz, B. Gallego, M.R. Kalu, E. Heyhawkins, R. Paschke, G.N. Kalu, Novel gallium (III) complexes containing phthaloyl derivatives of neutral aminoacids with apoptotic activity in cancer cells. *J. Organomet. Chem. J.* **694**, 2191–2197 (2009)
 4. K.C. Emregül, E. Düzgün, O. Atakol, The application of some polydentate Schiff base compounds containing aminic nitrogens as corrosion inhibitors for mild steel in acidic media. *Corros. Sci.* **48**, 3243–3260 (2006)
 5. M.A. Ashraf, A. Wajid, K. Mahmood, M.J. Maah, I. Yusoff, Spectral investigation of the activities of amino substituted bases. *Orient. J. Chem.* **27**, 363–372 (2011)
 6. A. Golcu, M. Tumer, H. Demirelli, and R. A. Wheatley, Cd(II) and Cu(II) complexes of polydentate Schiff base ligands: synthesis, characterization, properties and biological activity. *Inorg. Chim. Acta* **358**, 1785–1797 (2005)
 7. S. Mortazavi-Derazkola, S. Zinatloo-Ajabshir, M. Salavati-Niasari, New sodium dodecyl sulfate-assisted preparation of Nd₂O₃ nanostructures via a simple route. *RSC Adv.* **5**, 56666–56676 (2015)
 8. N. K. Yetim, E. H. Özkan, C. Özcan, N. Sarı, Preparation of AChE immobilized microspheres containing thiophene and furan for the determination of pesticides by the HPLC-DAD method. *J. Mol. Struct.* **1222**, 128931 (2020)
 9. Z. Parsaee, Sonochemical synthesis and DFT studies of nano novel Schiff base cadmium complexes: green, efficient, recyclable catalysts and precursors of Cd NPs. *J. Mol. Struct.* **1146**, 644–659 (2017)
 10. S. Zinatloo-Ajabshir, M. Emsaki, G. Hosseinzadeh, Innovative construction of a novel lanthanide cerate nanostructured photocatalyst for efficient treatment of contaminated water under sunlight. *J. Colloid Interface Sci.* **619**, 1–13 (2022)
 11. S. Zinatloo-Ajabshir, M. S. Morassaei, M. Salavati-Niasari, Eco-friendly synthesis of Nd₃Sn₂O₇-based nanostructure materials using grape juice as green fuel as photocatalyst for the degradation of erythrosine. *Composites Part B* **167**, 643–653 (2019)
 12. K. Mahdavi, S. Zinatloo-Ajabshir, Q.A. Yousif, M. Salavati-Niasari, Enhanced photocatalytic degradation of toxic contaminants using Dy₂O₃-SiO₂ ceramic nanostructured materials fabricated by a new, simple and rapid sonochemical approach. *Ultrason. Sonochem.* **82**, 105892 (2022)
 13. S.M. Tabatabaeinejada, S. Zinatloo-Ajabshir, O. Amiric, M. Salavati-Niasari, Magnetic Lu₂Cu₂O₅-based ceramic nanostructured materials fabricated by a simple and green approach for an effective photocatalytic degradation of organic contamination. *RSC Adv.* **11**, 40100–40111 (2021)
 14. S. Mortazavi-Derazkola, S. Zinatloo-Ajabshir, M. Salavati-Niasari, Preparation and characterization of Nd₂O₃ nanostructures via a new facile solvent-less route. *J. Mater. Sci.* **26**, 5658–5667 (2015)
 15. H. Ogutcu, S. Meral, S. Ceker, A.A. Agar, G. Agar, Determination of antimicrobial and antimutagenic properties of some Schiff bases. *An Acad Bras Cienc* **93**, 2–8 (2021)
 16. N.A. Naz, S. Arun, S.S. Narvi, M.S. Alam, A. Singh, P. Bhartiya, P.K. Dutta, Cu(II)-carboxymethyl chitosan-silane schiff base complex grafted on nano silica: structural evolution, antibacterial performance and dyedegradation ability. *Int. J. Biol. Macromol.* **110**, 215–226 (2018)
 17. E. Nadia Md Yusof, M. A. M. Latif, M. I. M. Tahir, J. A. Sakoff, M. I. Simone, Alister J. Page, A. Veerakumarasivam, E. R. T. Tiekink, and T. B. S. A. Ravooof, o-Vanillin derived schiff bases and their organotin(IV) compounds: synthesis, structural characterization, in-silico studies and cytotoxicity. *Int. J. Mol. Sci.* **20**, 854–862 (2019)
 18. A. Prakash, D. Adhikari, Application of Schiff bases and their metal complexes—a review. *Int. J. ChemTech Res.* **3**, 1891–1896 (2011)
 19. E.H. Özkan, N. Sarı, Use of immobilized novel dendritic molecules as a marker for the detection of glucose in artificial urine. *J. Mol. Struct.* **1201**, 127134 (2020)
 20. M. Grigoras, C.O. Catanescu, Imine oligomers and polymers. *J. Macromol. Sci. Part C* **C44**, 131–173 (2004)
 21. R. Rasool, S. Hasnain, N. Nishat, Metal-based Schiff base polymers: preparation, spectral, thermal and their in vitro biological investigation. *Des. Monomers Polym.* **17**, 217–226 (2014)
 22. D. Nartop, E.H. Ozkan, M. Gündem, S. Çeker, G. Ağar, H. Ögütücü, N. Sarı, Synthesis, antimicrobial and antimutagenic effects of novel polymeric- Schiff bases including indol. *J. Mol. Struct. J.* **1195**, 877–882 (2019)
 23. J. Zhao, Y. Xie, D. Guan, H. Hua, R. Zhong, Y. Qin, J. Fang, H. Liu, J. Chen, BaFe₁₂O₁₉-chitosan Schiff-base Ag(I) complexes embedded in carbon nanotube networks for high-performance electromagnetic materials. *Sci. Rep.* **5**, 1–11 (2015)
 24. E. Sonker, R. Tiwari, K. Kumar, S. Krishnamoorthi, Electrical properties of new polyazomethines. *SN Appl. Sci.* **2**, 1–12 (2020)
 25. J. Zhou, F. Gao, T. Jiao, R. Xing, L. Zhang, Q. Zhang, Selective Cu(II) ion removal from wastewater via surface charged self-assembled polystyrene-Schiff base nanocomposites. *Colloids Surf. A* **545**, 60–67 (2018)
 26. M.Y. Khuhawar, M.A. Mughal, A.H. Channar, Synthesis and characterization of some new Schiff base polymers. *Eur. Polym. J.* **40**, 805–809 (2004)
 27. C. O. Sánchez, J. C. Bèrnedè, L. Cattin, M. Makha, and N. Gatica, Schiff base polymer based on triphenylamine moieties in the main chain. Characterization and studies in solar cells. *Thin Solid Films* **562**, 495–500 (2014)
 28. D. Nartop, E.H. Özkan, N.K. Yetim, N. Sarı, Qualitative enzymatic detection of organophosphate and carbamate insecticides. *J. Environ. Sci. Heal. B* **55**, 951–958 (2020)
 29. E. Karmaz, E.H. Özkan, N.K. Yetim, N.B. Sarı, New nanospheres to use in the determination of imidan phosmet and vantex pesticides. *J. Inorg. Organomet. Polym. Mater.* **31**, 2915–2924 (2021)
 30. M. Cleiton, L. Daniel, L.V. Modolo, R.B. Alves, M.A. De Resende, C.V.B. Martins, Schiff bases: a short review of their antimicrobial activities. *J. Adv. Res.* **2**, 1–8 (2011)
 31. E. De Clercq, Strategies in the design of antiviral drugs. *Nat. Rev. Drug Discov.* **1**, 13–25 (2002)
 32. D. Nartop, B. Demirel, M. Güleç, E. H. Özkan, N. Kurnaz Yetim, N. Sarı, S. Çeker, H. Ögütücü, G. Ağar, Novel polymeric microspheres: synthesis, enzyme immobilization, antimutagenic activity, and antimicrobial evaluation against pathogenic microorganisms. *J. Biochem. Mol. Toxicol.* **34**, 1–13 (2019)
 33. N.K. Yetim, E.H. Özkan, B. Daniş, H. Tümtürk, N. Sarı, Research on the repeated use of novel ferrocene-tagged nanomaterial for determination of glucose. *Int. J. Polym. Mater. Polym. Biomater.* **64**, 888–893 (2015)
 34. A.S. El-tabl, K.Y. El-baradie, R.M. Issa, Novel platinum(II) and (IV) complexes of naphthaldimine schiff bases. *J. Coord. Chem.* **56**, 1113–1122 (2003)
 35. V. Torabi, H. Kargar, A. Akbari, R. Behjatmanesh-ardakani, H.A. Rudbari, M.N. Tahir, Nickel (II) complex with an asymmetric tetradentate Schiff base ligand: synthesis, characterization, crystal structure, and DFT studies. *J. Coord. Chem.* **71**, 3748–3762 (2018)
 36. X. Lu, Q. Xia, H. Zhan, H. Yuan, C. Ye, K. Su, G. Xu, Synthesis, characterization and catalytic property of tetradentate Schiff-base

- complexes for the epoxidation of styrene. *J. Mol. Catal. A Chem.* **250**, 62–69 (2006)
37. A.S. Altunçiqi, A.M.A. Alaghaz, R.A. Ammar, M.E. Zayed, Synthesis, spectral characterization, and thermal and cytotoxicity studies of Cr(III), Ru(III), Mn(II), Co(II), Ni(II), Cu(II), and Zn(II) complexes of schiff base derived from 5-hydroxymethylfuran-2-carbaldehyde. *J. Chem.* **3**, 1–17 (2018)
 38. D. Nartop, N.K. Yetim, E.H. Özkan, N. Sari, Enzyme immobilization on polymeric microspheres containing Schiff base for detection of organophosphate and carbamate insecticides. *J. Mol. Struct.* **1200**, 127039 (2020)
 39. S. Kundu, S. Biswas, A.S. Mondal, P. Roy, T.K. Mondal, Template synthesis of square-planar Ni(II) complexes with new thiophene appended Schiff base ligands: characterization, X-ray structure and DFT calculation. *J. Mol. Struct. J.* **1100**, 27–33 (2015)
 40. D. Nartop, Ö. Özdemir, P. Gürkan, Synthesis, characterization and investigation of tautomeric, potentiometric and antimicrobial properties of a novel unsymmetric Schiff base and its Fe(III) and Ni(II) complexes. *J. Chem.* **5**, 560–572 (2017)
 41. F.A. Cotton, G. Wilkinson, C.A. Murillo, M. Bochmann, R. Grimes, *Advanced Inorganic Chemistry*. Wiley, New York **6**, 1455 (1988)
 42. N.K. Singh, S.B. Singh, Complexes of 1-isonicotinoyl-4-benzoyl-3-thiosemicarbazide with manganese(II), iron(III), chromium(III), cobalt(II), nickel(II), copper(II) and zinc(II). *Transit. Met. Chem.* **26**, 487–495 (2001)
 43. A.A.A. Aziz, S.H. Seda, Synthesis, structural features and biochemical activity assessment of N, N'-bis-(2-mercaptophenylimine)-2,5-thiophenedicarboxaldehyde Schiff base and its Co(II), Ni(II), Cu(II) and Zn(II) complexes. *Organomet. Chem.* **31**, 1–12 (2017)
 44. D. Nartop, Ç. Kazak, Synthesis and characterization of novel polystyrene-silica composites containing azomethine. *J. Mol. Struct.* **1227**, 129705 (2021)
 45. D. Nartop, N. Sari, Novel Poly(styrene) attached schiff bases for uptake Mn(II) and Ni(II) ions and as antimicrobial agent against *Micrococcus luteus*. *J. Inorg. Organomet. Polym Mater.* **22**, 772–779 (2012)
 46. D. Nartop, N. Sari, A. Altundaş, H. Öğütçü, Synthesis, characterization, and antimicrobial properties of new polystyrene-bound Schiff bases and their some complexes. *J. Appl. Polym. Sci.* **125**, 1796–1803 (2012)
 47. A. Kotiranta, K. Lounatmaa, M. Haapasalo, Epidemiology and pathogenesis of *Bacillus cereus* infections. *Microbes Infect.* **2**, 189–198 (2000)
 48. J.P.S. Cabral, Water microbiology. Bacterial pathogens and water. *Int. J. Environ. Res. Public Health* **7**, 3657–3703 (2010)
 49. A.M. Spagnolo, M. Sartini, M.L. Cristina, *Pseudomonas aeruginosa* in the healthcare facility setting. *Rev. Med. Microbiol.* **32**, 169–175 (2021)
 50. H. Uslu, G. Şengül, O. Aktaş, A rare case of cranial osteomyelitis caused by *Proteus vulgaris*. *Balk. Med J.* **28**, 113–115 (2011)
 51. K.J. Ryan, C.G. Ray, *Sherris Medical Microbiology*, 4th edn. (McGraw-Hill, New York, 2004)
 52. P.C. Götzsche, H.K. Johansen, Nystatin prophylaxis and treatment in severely immunodepressed patients. *Cochrane Collab.* **4**, 1–19 (2014)
 53. N. Martins, I.C.F.R. Ferreira, L. Barros, S. Silva, M. Henriques, Candidiasis: predisposing factors, prevention, diagnosis and alternative treatment. *Mycopathologia* **177**, 223–240 (2014)
 54. W. Zhang, Y.H. Zhang, J.H. Ji, J. Zhao, Q. Yan, P.K. Chu, Antimicrobial properties of copper plasma-modified polyethylene. *Polymer* **47**, 7441–7445 (2006)
 55. K.H. Hong, G. Sun, Poly(styrene-co-vinylbenzophenone) as photoactive antimicrobial and self decontaminating materials. *J Appl Polym Sci.* **109**, 3173–3179 (2008)
 56. D. Nartop, E. Tokmak, E.H. Özkan, H.E. Kızıllı, H. Öğütçü, G. Açar, S. Allı, Synthesis of novel polymers containing Schiff base as potential antimutagenic and antimicrobial agents. *J. Med. Chem. Sci.* **4**, 363–372 (2020)

Publisher's Note Springer Nature remains neutral with regard to jurisdictional claims in published maps and institutional affiliations.

Authors and Affiliations

Eyüp Ülke¹ · Elvan Hasanoğlu Özkan²  · Dilek Nartop³ · Hatice Öğütçü⁴

¹ Department of Chemistry, Graduate School of Natural and Applied Sciences, Düzce University, Düzce, Turkey

² Department of Chemistry, Faculty of Science, Gazi University, Teknikokullar, 06500 Ankara, Turkey

³ Department of Chemistry, Faculty of Arts and Sciences, Düzce University, Düzce, Turkey

⁴ Department of Field Crops, Faculty of Agriculture, Kırşehir Ahi Evran University, Kırşehir, Turkey